RADIUS ANOMALY IN LOW-MASS ECLIPSING BINARIES FROM THE WTS

Patricia Cruz[1], Marcos Diaz[1], and Jayne Birkby[2].

1: Department of Astronomy, University of Sao Paulo (IAG/USP), Brazil; 2: Anton Pannekoek Institute for Astronomy, University of Amsterdam, The Netherlands; contact: patricia.cruz@usp.br

Abstract

Eclipsing binaries (EBs) provide a complete determination of their physical and orbital parameters when photometric and spectroscopic data are combined. Detached EBs also give the most precise ways to measure their fundamental properties, such as mass and radius, without the use of stellar evolutionary models. The majority of short-period low-mass eclipsing binaries from the literature present measured stellar radii that are usually 5 to 10% bigger than the expected values when compared to stellar models. This inflation trend is known as the radius anomaly of low-mass stars. We have characterized five short-period low-mass eclipsing binaries from the WFCAM Transit Survey (WTS). Photometric WFCAM J-mag data and additional low- and intermediate-resolution spectroscopic data were analyzed to obtain both orbital and physical properties of the studied systems. We modeled simultaneously light curves and radial velocity shifts with the JKTEBOP code, and performed MCMC simulations for the error estimates. The best-model fit have revealed that these detached binaries are in very close orbits, with short orbital periods of less than 2 days. The components of these systems have stellar masses between 0.24 and 0.72 Msun and radii ranging from 0.42 to 0.67 Rsun. The great majority of the low-mass stars in our sample has derived radii distant from the values predicted by evolutionary models, with an estimated radius inflation of 9% or more.

WTS: WFCAM Transit Survey

WTS was a survey awarded with 200 nights (and extended) with the Wide Field Camera (WFCAM) on the 4m UK Infrared Telescope (UKIRT) to search for planets via the transit method at infrared wavelengths. As a secondary outcome, a fine number of light curves of low-mass EBs was discovered with short periods of less than 5 days (Birkby et al. 2012). We have solved 5 low-mass eclipsing binary (LMEB) systems, with orbital period of less than 2 days, by modeling light curves and radial velocity shifts.

Characterizing the LMEB components

First approach: Spectral Energy Distribution (SED) fitting using VOSA (Bayo et al. 2008), considering filters SDSS ugriz, WFCAM ZYJHK, 2MASS JHKs, and WISE W1 W2.
Second approach: analyzing low-resolution spectra obtained with TWIN/3.5m-telescope from Calar Alto Observatory.

SED fitting

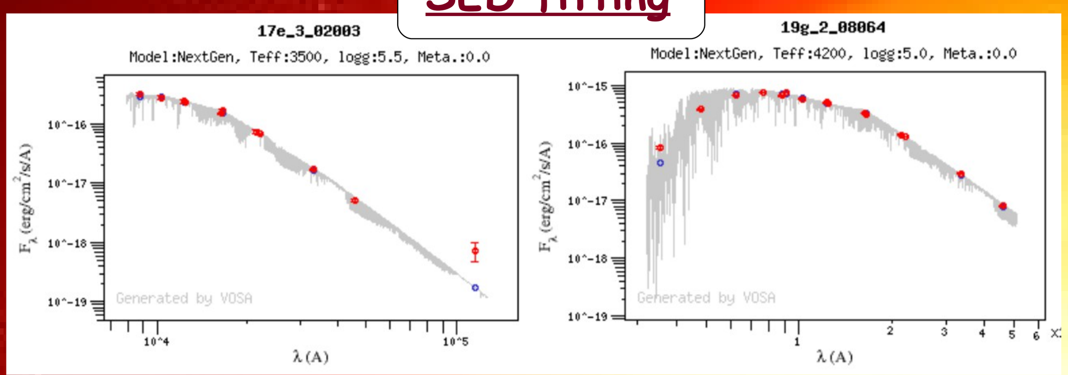

Spectral indices

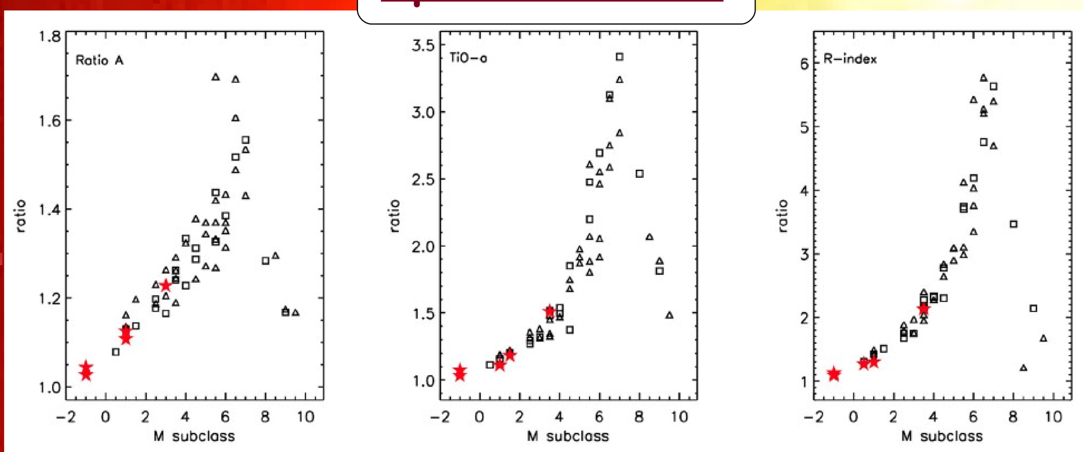

Spectral indices considered:
- Ratio A: 7020-7050 / 6960-6990 (Kirkpatrick et al. 1991)
- TiO-a: 7033-7048 / 7058-7073 (Kirkpatrick et al. 1999)
- R-TiO: 7485-7515 / 7120-7150 (Aberasturi et al. 2014)

Using 58 templates (Leggett et al. 2000; Cruz & Reid 2002).

Composite spectra

To estimate the effective temperature of each component individually, we compared the observed flux-calibrated low-resolution spectra to a combination of two BT-Settl synthetic spectra (Allard et al. 2013).

Synthetic spectra				
$T_{eff,1}$ (K)	$\log g_1$	$T_{eff,2}$ (K)	$\log g_2$	Type^b
3800	4.5	3500	4.5	M0+M2.5
3400	4.5	3200	5.0	M3+M4
3900	4.5	3000	4.5	M0+M5
4400	4.5	3500	5.0	K5+M2.5
4200	4.5	3100*	5.0	K6+M4.5*

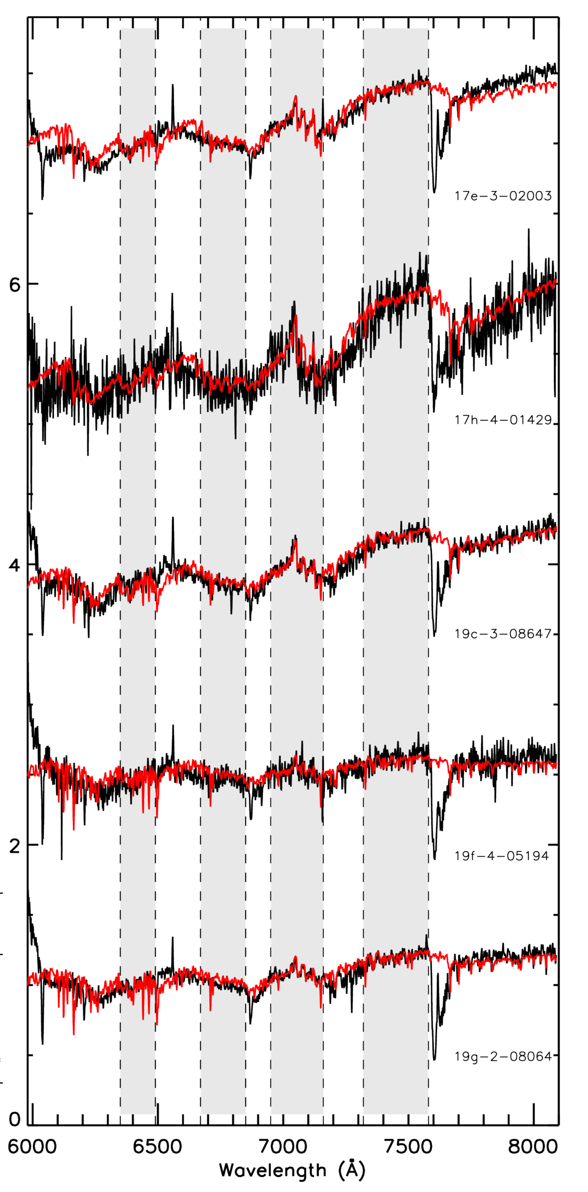

Solving the 5 LMEB systems

Radial Velocity Data

We also acquired intermediated resolution (R~10000) spectra with the TWIN/3.5m-telescope in order to measure radial velocity (RV) shifts. The RVs were obtained using the Ha emission line via Fourier cross-correlation with IRAF's FXCOR.

Modeling Photometric and Spectroscopic Data

We used the JKTEBOP code (Southworth et al. 2004, 2013) to analyze the photometric (LCs) and spectroscopic data (RVs) simultaneously to obtain an unique solution for each EB system.

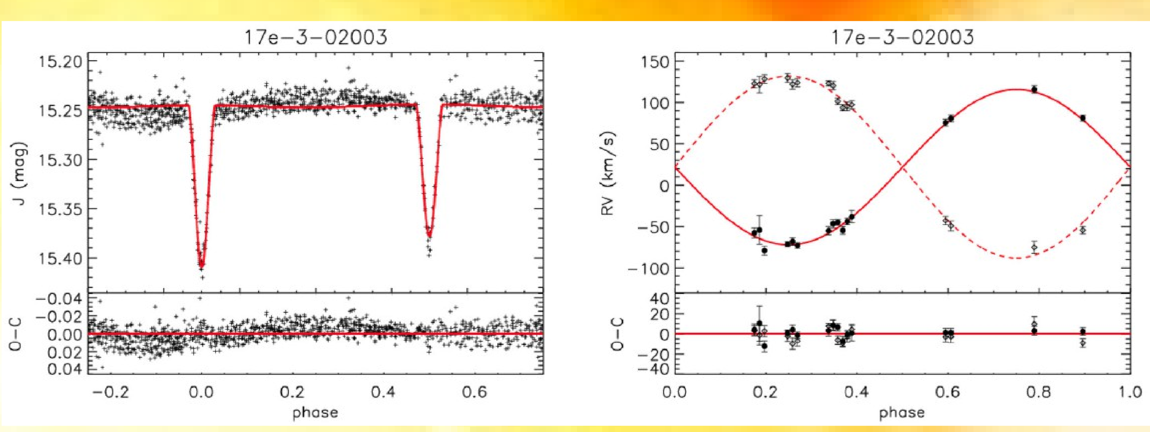

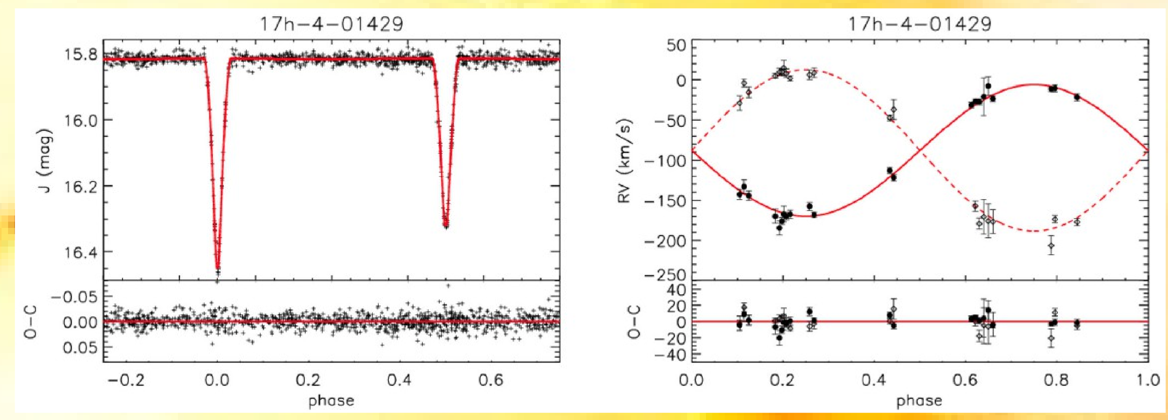

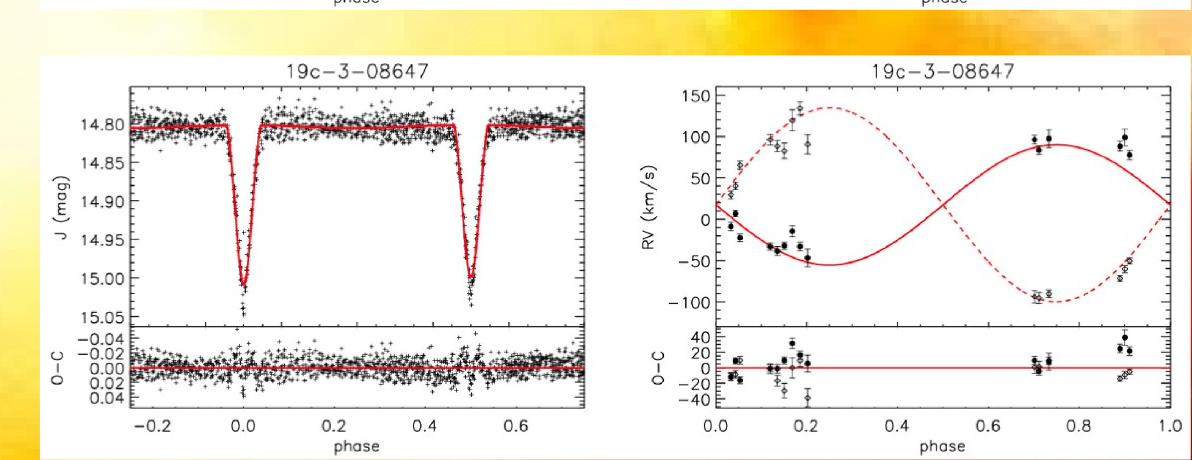

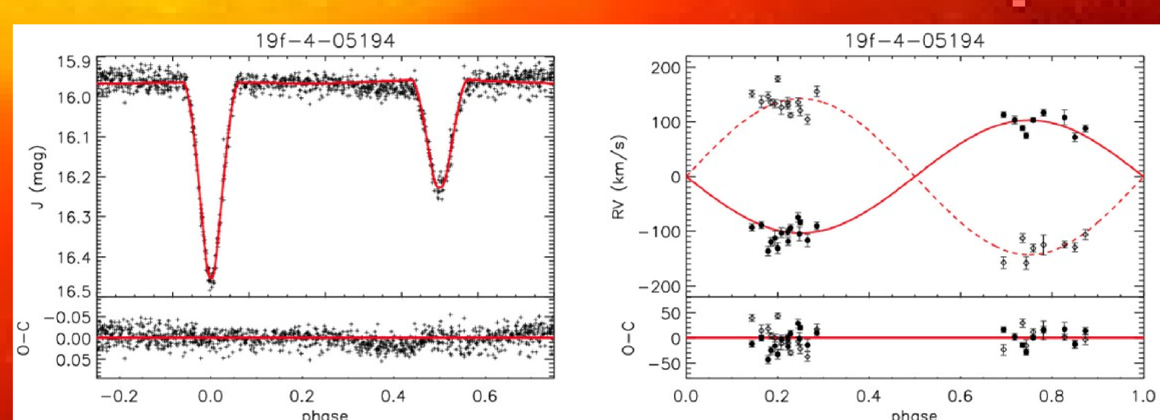

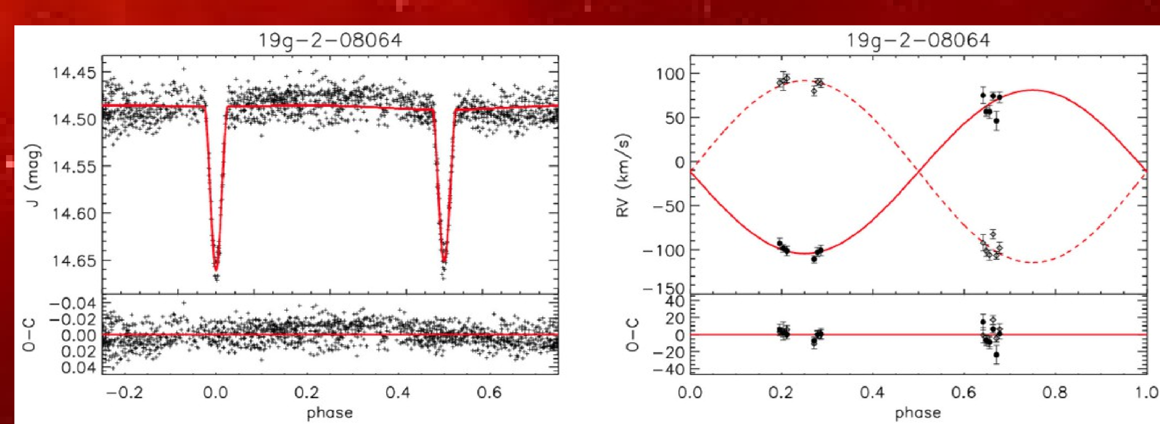

Results

Binary	17e-3-02003	17h-4-01429	19c-3-08647	19f-4-05194	19g-2-08064
FITTED PARAMETERS					
J	0.783 ± 0.028	0.8677 ± 0.0051	0.898 ± 0.027	0.5660 ± 0.0044	0.8492 ± 0.0111
$(R_1 + R_2)/a$	0.2304 ± 0.0048	0.17931 ± 0.00084	0.2783 ± 0.0038	0.3745 ± 0.0019	0.1955 ± 0.0021
k	0.88 ± 0.35	0.8189 ± 0.0081	0.86 ± 0.30	0.6531 ± 0.0048	0.95 ± 0.24
R_1/a	0.123 ± 0.019	0.09858 ± 0.00051	0.150 ± 0.021	0.2266 ± 0.0010	0.1002 ± 0.0117
R_2/a	0.108 ± 0.023	0.08073 ± 0.00070	0.128 ± 0.023	0.1480 ± 0.0013	0.0954 ± 0.0134
i (°)	81.77 ± 0.43	89.15 ± 0.13	81.29 ± 0.39	85.62 ± 0.20	83.33 ± 0.20
Light scale (mag)	15.2503 ± 0.0006	15.8191 ± 0.0003	14.8092 ± 0.0006	15.9724 ± 0.0004	14.4830 ± 0.0005
T_0 (MHJD−54000.) (d)	553.12520 ± 0.00027	553.15187 ± 0.00012	318.00600 ± 0.00010	317.60678 ± 0.00014	318.30802 ± 0.00015
P_{orb} (d)	1.2250078 ± 0.0000003	1.4445891 ± 0.0000002	0.86746584 ± 0.00000008	0.58953012 ± 0.00000008	1.7204091 ± 0.0000003
K_1 (km s^{-1})	93.80 ± 1.45	81.89 ± 1.15	72.70 ± 2.07	103.28 ± 1.40	92.56 ± 1.73
K_2 (km s^{-1})	109.93 ± 1.71	100.71 ± 1.43	117.19 ± 2.22	142.61 ± 1.81	102.99 ± 1.71
γ_{sys} (km s^{-1})	21.86 ± 1.01	−87.89 ± 0.79	17.37 ± 1.03	−0.33 ± 1.07	−11.63 ± 1.15
ABSOLUTE DIMENSIONS					
L_2/L_1	0.62 ± 0.60	0.584 ± 0.011	0.69 ± 0.58	0.264 ± 0.004	0.84 ± 0.43
a ($R_\odot$)	4.982 ± 0.049	5.212 ± 0.053	3.292 ± 0.054	2.872 ± 0.027	6.692 ± 0.082
q	0.853 ± 0.020	0.813 ± 0.016	0.620 ± 0.021	0.724 ± 0.013	0.899 ± 0.023
M_1 ($M_\odot$)	0.597 ± 0.020	0.503 ± 0.016	0.393 ± 0.019	0.531 ± 0.016	0.717 ± 0.027
M_2 ($M_\odot$)	0.510 ± 0.016	0.409 ± 0.013	0.244 ± 0.014	0.385 ± 0.011	0.644 ± 0.025
R_1 ($R_\odot$)	0.611 ± 0.095	0.514 ± 0.006	0.494 ± 0.069	0.651 ± 0.007	0.670 ± 0.078
R_2 ($R_\odot$)	0.54 ± 0.11	0.421 ± 0.006	0.422 ± 0.077	0.425 ± 0.006	0.638 ± 0.090
$\log g_1$	4.64 ± 0.14	4.717 ± 0.008	4.65 ± 0.13	4.536 ± 0.007	4.64 ± 0.10
$\log g_2$	4.69 ± 0.18	4.801 ± 0.010	4.57 ± 0.16	4.766 ± 0.009	4.64 ± 0.13
ρ_1 (g cm^{-3})	2.6 ± 1.6	3.706 ± 0.067	3.3 ± 1.8	1.928 ± 0.030	2.38 ± 0.83
ρ_2 (g cm^{-3})	3.3 ± 2.2	5.49 ± 0.16	3.2 ± 1.8	5.01 ± 0.14	2.5 ± 1.3
$\log L_1$ ($L_\odot$)	−1.15 ± 0.14	−1.497 ± 0.052	−1.29 ± 0.13	−0.844 ± 0.040	−0.90 ± 0.11
$\log L_2$ ($L_\odot$)	−1.41 ± 0.19	−1.776 ± 0.056	−1.88 ± 0.17	−1.611 ± 0.051	−1.47 ± 0.21
$M_{bol,1}$ (mag)	7.63 ± 0.36	8.49 ± 0.13	7.98 ± 0.32	6.86 ± 0.10	7.00 ± 0.28
$M_{bol,2}$ (mag)	8.27 ± 0.48	9.19 ± 0.14	9.46 ± 0.42	8.78 ± 0.13	8.42 ± 0.52
d (pc)	875 ± 117	805 ± 62	571 ± 66	1400 ± 118	731 ± 75

The Mass-Radius Diagram

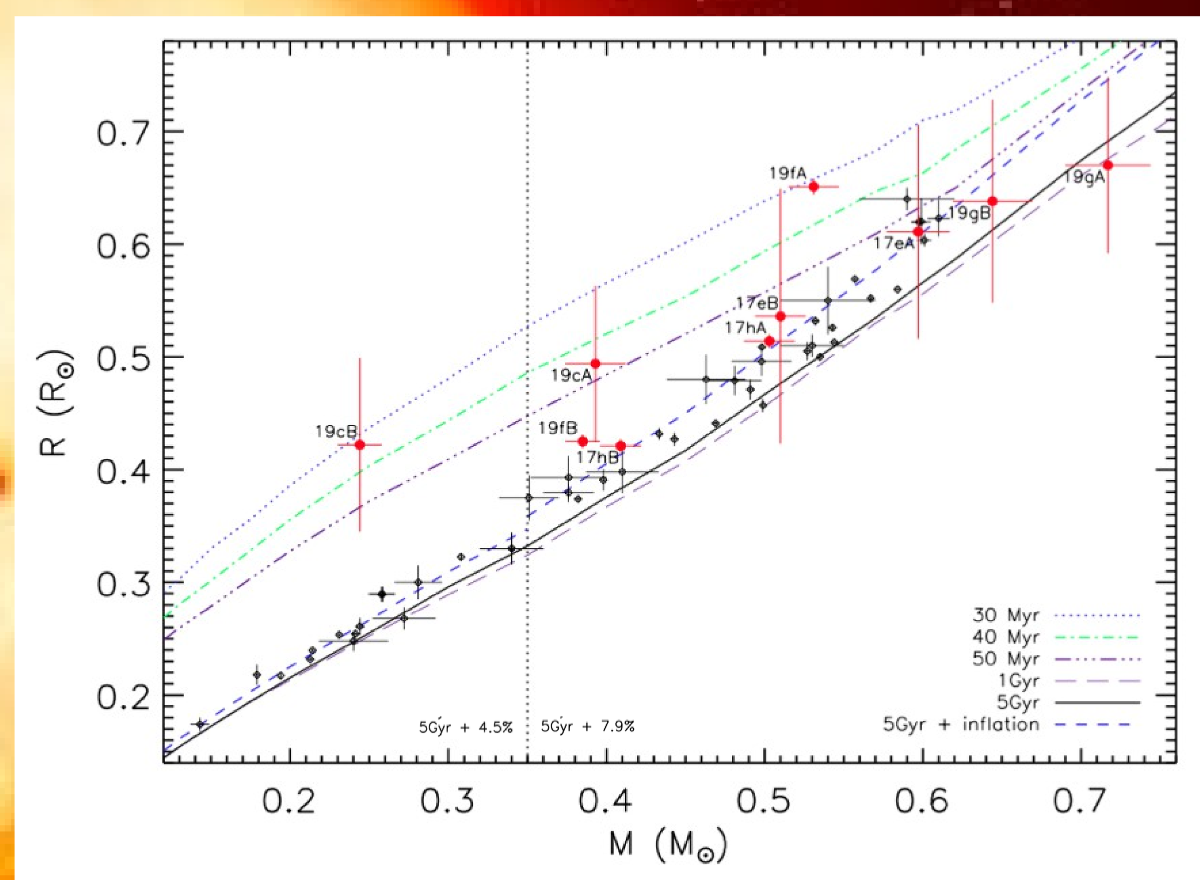

Our well-characterized EBs:
- 17h-4-01429A and 17h-4-01429B have an estimated radius inflation of around 9.4 and 9.9% when compared to the 5 Gyr model.
- 19f-4-05194A and 19f-4-05194B where we estimated 31.1 and 17.2% inflation. Similar to KELTJ041621-620046 (Lubin et al. 2017) that seems to have such radius anomaly, which are 28 and 17% inflated, respectively.

Despite radius uncertainties:
- 17e-3-02003A and B also present inflation of 8.6 and 12.5%, respectively.
- EB 19c-3-08647 is the less massive binary, and yet with the most inflated components in our sample, with 33.6 and 68.6% of inflation. Nevertheless, this EB seems to be a much younger system (~40 Myr), which would justify the observed inflation.
- The most massive binary in the sample is less or possibly not inflated. 19g-2-08064A does not show any inflation when compared to the 1 Gyr model, and 19g-2-08064B is only 6% inflated.

The great majority of the LMEB components has an estimated radius far from the predicted values according to evolutionary models, where the studied low-mass stars seem to be significantly inflated.

Discussion

We have observed a radius anomaly in the majority of the components of the studied LMEB systems, where the measured radius is greater than the value estimated from evolutionary models. The components with derived masses of less than 0.6 Msun present a radius inflation greater than 9%. This result supports the idea of a global trend of inflation of around 8% for partially-radiative stars (M > 0.35 Msun), as discussed by Knigge et al. (2011), for low-mass stars in close detached low-mass binary systems. Such short-period systems should be synchronized and circularized (Zahn 1977) and, according to Chabrier et al. (2007), this would enhance their magnetic activity enhancement and reduced the convective efficiency, leading to more inflated stars. This hypothesis is supported by observed Ha and X-ray emission. The systems presented here, which results are fully published in Cruz et al. (2018), add to the increasing sample of low-mass stars that are not explained by present stellar models. They highlight the importance of new studies on the role of magnetic activity in cool stars and the need for a greater sample of model-independent well-characterized LMEBs.

References: Aberasturi, M. et al., 2014, AJ, 148, 36; Allard, F. et al., 2013, MSAIS, 24, 128; Bayo, A. et al., 2008, A&A, 492, 277; Birkby, J. et al., 2012, MNRAS, 417, 709; Chabrier G., Gallardo J., Baraffe I., 2007, A&A, 472, L17; Cruz K. L., Reid I. N., 2002, AJ, 123, 2828; Cruz, P. et al., 2018, MNRAS, 476, 4, 5253; Kirkpatrick, J. et al., 1991, ApJS, 77, 417; Kirkpatrick, J. et al., 1999, ApJ, 519, 834; Knigge C., Baraffe I., Patterson J., 2011, ApJS, 194, 28; Leggett, S. et al., 2000, ApJ, 535, 965; Lubin J. B. et al., 2017, ApJ, 844, 134; Southworth, J. et al., 2004, MNRAS, 351, 1277; Southworth, J. et al., 2013, A&A, 557, A119; Zahn J.-P., 1977, A&A, 57, 383.